

## THERMODYNAMIC DESCRIPTION OF THE Mg-O AND Al-O SYSTEMS

X.-J. Li, S.-H. Liu\*

Central South University, National Key Laboratory of Science and Technology on High-strength Structural Materials, Changsha, Hunan, China

(Received 21 June 2023; Accepted 04 December 2023)

### Abstract

The thermodynamic properties of oxides have a considerable influence on the corrosion behavior of alloys. MgO and Al<sub>2</sub>O<sub>3</sub> are important products in the corrosion process of Mg-Al alloys, therefore it is necessary to investigate their thermodynamic properties. The Mg-O and Al-O systems were critically evaluated and re-evaluated using the CALPHAD (CALculation of PHase Diagram) approach. The liquid phases of these systems were described using the ionic liquid model. According to the literature data, the oxide phases, MgO and Al<sub>2</sub>O<sub>3</sub> were treated as stoichiometric compounds. The thermodynamic parameters of the two stoichiometric compounds were optimized considering both the phase diagram and the thermodynamic data, and finally a set of self-consistent thermodynamic parameters was determined for each system. The calculated results using the presently obtained thermodynamic parameters can reasonably reproduce the reliable experimental data in the literature.

**Keywords:** Mg-O; Al-O; Thermodynamic evaluation; Phase diagram; CALPHAD method

### 1. Introduction

Magnesium alloys have gained more and more attention in automobiles, aerospace, electronic products, and biomedical materials [1-5] due to their advantages of low density, high strength, good castability, and excellent biocompatibility. However, the poor corrosion resistance greatly limits their application in various fields [6-9]. It has been reported that the oxide films naturally formed on the surface of magnesium alloys play an important role in the corrosion performance of the alloys [10-13]. To improve the corrosion resistance of the alloys, many researchers tried to adjust the chemical composition and microstructure of the oxide films by adding alloying elements. Al is one of the most commonly used alloying elements. MgO and Al<sub>2</sub>O<sub>3</sub> are usually formed in the corrosion products when Al is added to Mg alloys [14,15].

Knowledge of phase equilibria is crucial for understanding the stability of the constituent phases of a given material and providing guidance on analyzing the performance of the materials. Accurate description of binary and ternary systems is an important part of calculating phase equilibria and thermodynamic properties in multi-component systems. The CALPHAD (CALculation of PHase Diagram) approach is a useful tool to establish thermodynamic databases. Therefore, to better understand the effect of

the corrosion products on the corrosion performance of Mg-Al alloys, it is necessary to obtain an accurate thermodynamic database of Mg-Al-O system. To construct the entire ternary Mg-Al-O system, it is essential to have thermodynamic descriptions of the constituent binary systems, including Mg-Al, Mg-O and Al-O. The Mg-Al system has been evaluated and assessed by several researchers [16-18] and the thermodynamic description of this system has been constructed well. However, the thermodynamic descriptions for Mg-O and Al-O systems still needs improvements.

Critical literature review of Mg-O and Al-O systems have been carried out by Wriedt [19, 20]. The Mg-O system has been assessed by several groups [21-23] using different thermodynamic models. Using ionic liquid model, Hallstedt [21] obtained a set of thermodynamic parameters of the Mg-O system. Then, the Mg-O system was re-optimized by Liang and Schmid-Fetzer [22] using the associated solution model. Based on the thermodynamic parameters of Hallstedt [21], Ma et al. [23] re-assessed the parameters of MgO to investigate the diffusion kinetics. Chernyshev et al. [24] and Ronchi and Sheindlin [25] re-determined the melting point of MgO which were about 150 K higher than the previous experimental [26-29] and calculated results [21,23]. Although Liang and Schmid-Fetzer [22] using the new melting point data but the solubility of

Corresponding author: shhliu@csu.edu.cn

<https://doi.org/10.2298/JMMB230621034L>



O in liquid metal in their work was different from those evaluated by Wriedt [19] and Hallstedt [21]. Therefore, considering the solubility of O in Mg and the melting point of MgO, the Mg-O system needs a further optimization. The Al-O system has been assessed by three groups [30-32] using the ionic liquid model. Thermodynamic parameters of the gas phase reported by Taylor et al. [30] have been updated in SGTE substances database [33]. Mao et al. [31] re-optimized the thermodynamic parameters of the Al-O system using the updated thermodynamic parameters of the gas phase. However, they neglected the solubility of O in liquid Al. Based on assessed result of Mao et al. [31], Ta et al. [32] re-optimized the parameters of  $\text{Al}_2\text{O}_3$  to investigate the diffusion kinetics. In their optimization,  $\text{Al}_2\text{O}_3$  has a solid solubility range rather than a stoichiometric compound, but there are no experimental results to support the calculated result. Therefore, thermodynamic parameters of the Al-O system still need further investigation. The purpose of the present work is to obtain reasonable thermodynamic parameters for describing the Mg-O and Al-O systems.

## 2. Literature review

The available literature data of the X-O (X = Mg, Al) systems, including phase diagram and thermodynamic data, were critically reviewed in present work and summarized in Tables 1 and 2.

**Table 1.** Reported crystal structure of the X-O systems in literature

Mg-O [19]				
Phase	Pearson symbol	Space group	Prototype	Strukturbericht symbol
Hcp_A3	hP2	$P6_3/mmc$	Mg	A3
MgO	cF8	Fm3m	NaCl	B1
$\text{MgO}_2$	cP12	Pa3	$\text{FeS}_2$	C2
Al-O [20]				
Fcc_A1	cF4	Fm3m	Cu	A1
$\text{Al}_2\text{O}_3$	hR10	$R\bar{3}c$	$\text{Al}_2\text{O}_3$	D5 <sub>1</sub>

### 2.1. Phase diagram data

#### 2.1.1. Mg-O system

Five magnesium oxides,  $\text{Mg}_2\text{O}$ , MgO,  $\text{MgO}_2$ ,  $\text{MgO}_4$ , and  $\text{MgO}_6$  have been reported in literature and evaluated by Wriedt [19] for the Mg-O system. The crystal structure of the phases was summarized in Table 1.

$\text{Mg}_2\text{O}$  was reported by Minami et al. [34] on the oxidized surfaces of Mg particles dispersed in molten

mixtures of  $\text{MgCl}_2$  and KCl at 1073 to 1173 K. However, the stability of this phase needs further research. Schwitzgebel and Lowell [35] proposed the possible existence of equilibrium  $\text{MgO} + \text{O}_2 = \text{MgO}_2$  in terms of thermodynamics. However, it was not proved by subsequent experiments and several researchers were skeptical about the deduction of Schwitzgebel and Lowell [35]. Therefore,  $\text{MgO}_2$  and the possible equilibrium were not considered in the present work. Vol'nov et al. [26] reported that the  $\text{MgO}_4$  phase was unstable at atmospheric pressure and temperatures above about 243 K. The existence of  $\text{MgO}_6$  was reported by Blumenthal [27], but this result was disputed by Vol'nov [28].

Considering the above references, only MgO was considered in the present assessment. The melting point of MgO has been reported by several groups. Using optical pyrometer, Ruff [29] obtained various melting points (2423 to 2872 K) that were measured in differently shaped specimens. By the same method, Kanolt [36] and McNally et al. [37] determined it to be  $3073 \pm 20$  K and  $3098 \pm 20$  K, respectively. Utilized the graphite resistance tube, it was measured to be  $3073 \pm 20$  K by Riley [38]. By means of pyrometer and high-speed spectropycrometer, it was determined by Chernyshev et al. [24] and Ronshi and Sheindlin [25] to be  $3215 \pm 30$  K and  $3250 \pm 20$  K, respectively. The measurement from Ronchi and Sheindlin [25], which was adopted by Liang and Schmid-Fetzer [22], was also accepted in the present work.

#### 2.1.2. Al-O system

Czochralski [39] introduced oxygen during the casting of aluminum, and then estimated the solubility of O in aluminum based on the volume of pores observed in the cast alloys. Obviously, the solubility of O in Al measured by this method is inaccurate. Several groups [40-45] also determined the content of O dissolved in Al to be the range from 0.0002 to 0.03 at.% O. However, the conditions for materials



**Table 2.** Summary of the experimental data in the X-O (X= Mg, Al) systems

Type of experimental data	Experimental technique	T(K)	Quoted mode <sup>a</sup>	Ref.
Melting point of MgO	OP	2423 to 2872	☒	[29]
Melting point of MgO	OP	3073	☒	[36]
Melting point of MgO	OP	3098±20	☒	[37]
Melting point of MgO	GRT	3073±20	☒	[38]
Melting point of MgO	HSS	3215±30	☒	[24]
Melting point of MgO	HSS	3250±20	☑	[25]
Enthalpy of formation of MgO	CC	298.15	☒	[72]
Enthalpy of formation of MgO	SC	298.15	☑	[73]
Enthalpy of formation of MgO	CC	298.15	☑	[74]
Heat capacity of MgO	BIC	373 to 1173	☑	[75]
Melting point of Al <sub>2</sub> O <sub>3</sub>	OP	2293	☒	[47]
Melting point of Al <sub>2</sub> O <sub>3</sub>	OP	2283	☒	[29]
Melting point of Al <sub>2</sub> O <sub>3</sub>	TA	2323	☒	[48]
Melting point of Al <sub>2</sub> O <sub>3</sub>	OP	2163	☒	[49]
Melting point of Al <sub>2</sub> O <sub>3</sub>	OP	2278	☒	[50]
Melting point of Al <sub>2</sub> O <sub>3</sub>	OP	2328	☒	[51]
Melting point of Al <sub>2</sub> O <sub>3</sub>	OP	2318	☒	[52]
Melting point of Al <sub>2</sub> O <sub>3</sub>	OP	2280	☒	[53]
Melting point of Al <sub>2</sub> O <sub>3</sub>	OP	2308	☒	[54]
Melting point of Al <sub>2</sub> O <sub>3</sub>	OP	2273-2303	☒	[55]
Melting point of Al <sub>2</sub> O <sub>3</sub>	OP	2307	☒	[56]
Melting point of Al <sub>2</sub> O <sub>3</sub>	OP	2322	☒	[57]
Melting point of Al <sub>2</sub> O <sub>3</sub>	TA	2333	☒	[58]
Melting point of Al <sub>2</sub> O <sub>3</sub>	OP	2293	☒	[59]
Melting point of Al <sub>2</sub> O <sub>3</sub>	OP	2298	☒	[60]
Melting point of Al <sub>2</sub> O <sub>3</sub>	OP	2316	☒	[37]
Melting point of Al <sub>2</sub> O <sub>3</sub>	OP	2317	☒	[37]
Melting point of Al <sub>2</sub> O <sub>3</sub>	-	2343	☒	[62]
Melting point of Al <sub>2</sub> O <sub>3</sub>	OP	2323	☒	[63]
Melting point of Al <sub>2</sub> O <sub>3</sub>	TA	2315	☒	[64]
Melting point of Al <sub>2</sub> O <sub>3</sub>	TA	2314	☒	[65]
Melting point of Al <sub>2</sub> O <sub>3</sub>	TA	2322.7	☒	[66]
Melting point of Al <sub>2</sub> O <sub>3</sub>	TA	2310	☒	[67]
Melting point of Al <sub>2</sub> O <sub>3</sub>	TA	2320	☒	[68]
Melting point of Al <sub>2</sub> O <sub>3</sub>	TA	2324±6 K	☑	[69]
Enthalpy of formation of Al <sub>2</sub> O <sub>3</sub>	CC	298.15	☑	[74]
Enthalpy of formation of Al <sub>2</sub> O <sub>3</sub>	CC	298.15	☑	[76]
Enthalpy of formation of Al <sub>2</sub> O <sub>3</sub>	EMF	298.15	☑	[77]
Enthalpy of formation of Al <sub>2</sub> O <sub>3</sub>	CC	298.15	☑	[78]
Heat capacity of Al <sub>2</sub> O <sub>3</sub>	BIC	323 to 1173	☑	[79]

OP-Optical Pyrometer; GRT- Graphite Resistance Tube; HSS- High-Speed Spectropyrometer; CC- Combustion Calorimetry; SC- Solution Calorimetry; BIC- Bunsen Ice Calorimeter; TA-Thermal Analysis

<sup>a</sup>indicates whether the data are used or not in the parameter optimization: ☑ used; ☒ not used.



preparation and testing were not clear. Wriedt [20] evaluated the available measured O solubility in Al in literature and concluded that the experimental data were relatively scattered. Based on the relationship between the enthalpy/entropy of O in various liquid metals and the formation of stable crystalline oxides, Otsuka and Kozuka [46] derived an empirical formula for calculating the solubility of O in liquid metals, which was adopted by Wriedt [20] and also considered in the present work.

Using the optical pyrometer and thermal analysis, the melting point of  $\text{Al}_2\text{O}_3$  has been determined by several researchers [29,37,47-69]. However, due to the purity of the raw materials and the influence of the experimental environments, the measured melting points differed from each other. Schneider and McDaniel [69] determined the melting point of  $\text{Al}_2\text{O}_3$  in an induction furnace under vacuum conditions. The purity of the samples used in the measurement was 99.9 wt.% and the obtained melting point was  $2324 \pm 6$  K, which was adopted by most researchers [20,70,71] and the present work.

## 2.2. Thermodynamic data

### 2.2.1. Mg-O system

Thermodynamic data of the Mg-O system were focused on enthalpy of formation and heat capacity of MgO. Using combustion calorimetry, Moose and Parr [72] determined the enthalpy of formation to be  $-304.88$  kJ/mol-atoms. Using solution calorimetry, Shomate and Huffman [73] determined the enthalpy of formation to be  $-300.8 \pm 0.11$  kJ/mol-atoms. By the same method used by Moose and Parr [72], Holley and Huber [74] determined the enthalpy of formation to be  $-300.43 \pm 0.25$  kJ/mol-atoms. The data obtained from Shomate and Huffman [73] and Holley and Huber [74] were consistent with each other and thus were considered in the present work. The heat capacity of MgO measured by Victor and Douglas [75] in a Bunsen ice calorimeter was also considered in the present work. The low temperature (up to 298.15 K) heat capacity data has been summarized by Chase et al. [70], and the standard entropy derived from heat capacity was  $26.924 \pm 0.08$  J/mol·K.

### 2.2.2. Al-O system

Several investigators reported the thermodynamic data of the Al-O system up to now. Utilized calorimetric heats of combustion, Mah [76] and Holley and Huber [74] measured the enthalpy of formation of the  $\text{Al}_2\text{O}_3$  to be  $-335.14 \pm 0.21$  kJ/mol-atoms and  $-335.14 \pm 0.25$  kJ/mol-atoms, respectively. Utilizing the EMF method, Sterten et al. [77] reported the enthalpy of formation of  $\text{Al}_2\text{O}_3$  to be  $-334.89 \pm 0.33$  kJ/mol-atoms. Using heat of combustion method,

Zenkov [78] determined the enthalpy of formation of  $\text{Al}_2\text{O}_3$  to be a range lower than  $-334.64$  kJ/mol-atoms. Using a Bunsen ice calorimeter, Ditmars and Douglas [79] measured the heat capacity and heat content of  $\text{Al}_2\text{O}_3$  in the temperature range of 273.15 K to 1173.15 K. Using an adiabatic receiving calorimeter, Ditmars et al. [80] determined the heat capacity and heat content of  $\text{Al}_2\text{O}_3$  in the temperature range of 1173.15 K to 2250 K and smoothed the heat capacity data using a least-squares spline technique from 10 K to near the melting point, which was accepted by Wriedt [20] and the present work.

## 3. Thermodynamic models

### 3.1. Unary phases

The Gibbs energy function  $G_i^{0,\phi}(T) = G_i^\phi(T) - H_i^{SER}$  of pure element  $i$  ( $i = \text{Mg, Al, or O}$ ) was taken from the SGTE compilation by Dinsdale [81] and described by the following equation:

$$G_i^{0,\phi}(T) = G_i^\phi(T) - H_i^{SER} = a + b \cdot T + c \cdot T \cdot \ln T + d \cdot T^2 + e \cdot T^3 + f \cdot T^{-1} + g \cdot T^7 + h \cdot T^{-9} \quad (1)$$

where  $H_i^{SER}$  is the molar enthalpy of the element  $i$  ( $i = \text{Mg, Al, O}$ ) at 1 bar and 25 °C in its standard element reference (SER) state, and  $T$  is the absolute temperature. The last two terms in Eq. (1) are used only outside the ranges of the melting point,  $gT^7$  for a liquid below the melting point and  $hT^{-9}$  for solid phases above the melting point.

### 3.2. Liquid phase

The liquid phase in these systems were described by the two sub-lattice model [82,83]. This model assumed that cations and anions form different sub-lattices and can mix freely in their respective sub-lattices. Hypothetical vacancies were introduced on the anion sub-lattice in order to extend the description to a liquid with only cations (a metallic liquid). The model can be written as:

$$(C_i^{v_i})_p (A_i^{v_i}, Va^{v_i})_q \quad (2)$$

where  $C$ ,  $A$  and  $Va$  represent cations, anions and hypothetical vacancies, respectively. The charge of an ion is denoted  $v_i$  and the index  $i$  is used to denote a specific constituent. The number of sites on the sub-lattices,  $p$  and  $q$ , must vary with the composition in order to maintain electroneutrality. The value of  $p$  and  $q$  are calculated from the following equations:

$$p = \sum_i (-v_i) y_{A_i} + q y_{Va} \quad (3)$$

$$q = \sum_i v_i y_{C_i}$$

where  $y$  denotes the site fraction of a constituent;



p and q are simply the average charge on the opposite sub-lattice. The hypothetical vacancies have an induced charge equal to q.

Take the Mg-O system as an example, the sub-lattice of the liquid phase can be written as  $(Mg^{2+})_2(O^{2-}, Va^{2-})_2$ . In this model, the liquid Mg is represented by the case when there are only vacancies on the second sub-lattice and liquid MgO when there is only oxygen. The Gibbs energy of the liquid phase in Mg-O system is given by:

$$G_m = 2y_{Va^{2-}} {}^0G_{MgVa} + y_{O^{2-}} {}^0G_{Mg_2O_2} + 2RT(y_{Va^{2-}} \ln y_{Va^{2-}} + y_{O^{2-}} \ln y_{O^{2-}}) + 2y_{Va^{2-}} y_{O^{2-}} L_{Mg^{2+}, O^{2-}, Va^{2-}} \quad (4)$$

### 3.3. Oxide phases

Two metal oxides, MgO and  $Al_2O_3$ , were considered as stoichiometric compounds and modeled using the following expression:

$$G_m^{X_i O_b} - A \cdot H_X^{SER} - B \cdot H_O^{SER} = a + b \cdot T + c \cdot T \cdot \ln T + dT^2 + eT^{-1} \quad (5)$$

where the coefficients *c*, *d*, and *e*, are obtained from the expression of heat capacity.

### 3.4. Gas phase

The gas phases were described as ideal gas mixtures of the species and their Gibbs energy per mol of species in the gas is given by:

$$G_m^{gas} - H^{SER} = \sum y_i (G_i^{gas} - H_i^{SER} + R \cdot T \cdot \ln y_i) + R \cdot T \cdot \ln(10^{-5} \cdot P) \quad (6)$$

where  $y_i$  is the mole fraction of species *i*, and *P* the pressure in Pa. The Gibbs energy functions for the individual gas species are taken from SGTE substance database [33].

## 4. Results and discussion

### 4.1. First-principles calculations

The obtained enthalpies of formation by first-principles calculations were compared with the data from Open Quantum Materials Database and Materials Project, as shown in Table 3. In the present work, the crystal structure CIF files for the first-principles calculations were downloaded from the website <http://www.crystallography.net/cod/> [84]. The first-principles calculations were performed based on density functional theory (DFT) [85,86] and plane-wave Vienna ab-initio simulation package (VASP) [87,88]. The interactions between ions and electrons were realized with the projector-augmented wave

(PAW) method [89] and the exchange-correlation functional items were expressed by generalized gradient approximation (GGA) refined by Perdew, Burke, and Ernzerhof (PBE) [90]. The cutoff energy for plane waves was selected as 250 eV after convergence in present work. The k points in the first irreducible Brillouin zone were the same  $13 \times 13 \times 13$  for MgO and  $Al_2O_3$ . As a result, the calculated enthalpies of formation were -281.86 kJ/(mol-atoms) for MgO, and -294.24 kJ/(mol-atoms) for  $Al_2O_3$ . It can be concluded that the calculated results were similar to the data from Materials Project.

**Table 3.** Calculated enthalpy of formation by first-principle method

	Calculated result in the present work (kJ/mol-atoms)	Data from the Open Quantum Materials Database (kJ/mol-atoms)	Data from Materials Project (kJ/mol-atoms)
MgO	-281.86	-282.82	-263.71
$Al_2O_3$	-294.24	-313.44	-329.86

### 4.2. Thermodynamic Calculations

The PARROT module of the Thermo-Calc software [91] was used to perform the optimization of thermodynamic parameters. The reliable experimental data summarized in Table 2 were considered in the optimization. Based on the reliability of the data, the experimental phase diagram data and thermodynamic properties were given a certain weight. The step-by-step optimization procedure carefully described by Du et al. [92,93] was utilized in the present work. Firstly, the optimization began with the oxides, MgO and  $Al_2O_3$  for Mg-O and Al-O system, respectively. The parameter *a* for both phases was optimized by the enthalpies of formation, while parameter *b* for both phases was determined by the standard entropy at 298.15 K. The heat capacities data were utilized to adjust the parameters *c*, *d*, and *e*. Second, the parameters for liquid MgO and  $Al_2O_3$  were determined based on the melting point of the solid oxides and the interaction parameters were adjusted by considering the solubility of O in liquid. Finally, all the parameters were optimized simultaneously based on the experimental data, and a set of self-consistent thermodynamic parameters for each system were obtained and the parameters for the two systems are presented in Table 4.

Table 5 shows the enthalpy of formation data in tabular form and also include data on standard entropy, heat capacity at 298.15 K, enthalpy of melting, and heat capacity of the liquid oxide. Figure 1 presents the calculated phase diagram of the Mg-O system, enthalpy of formation and heat capacity of the



**Table 4.** Thermodynamic parameter of the Mg-O and Al-O systems

<b>Mg-O system</b>	
Liquid: Model (Mg <sup>2+</sup> ) <sub>p</sub> (O <sup>2-</sup> , Va) <sub>q</sub>	
${}^0G_{Mg^{2+}:O^{2-}}^L - 2H_{Mg}^{SER} - 2H_O^{SER} = -1105134.7 + 854 * T - 133.88 * T * LN(T)$	
MgO: Model (Mg <sup>2+</sup> )(O <sup>2-</sup> )	
${}^0G^{MgO} - H_{Mg}^{SER} - H_O^{SER} = -618909.89 + 295.7 * T - 47.31 * T * LN(T)$ $-2.18E-3 * T^{**2} + 502493.16 * T^{**}(-1)$	
<b>Al-O system</b>	
Liquid: Model (Al <sup>3+</sup> ) <sub>p</sub> (O <sup>2-</sup> , Va) <sub>q</sub>	
${}^0G_{Al^{3+}:O^{2-}}^L - 2H_{Al}^{SER} - 3H_O^{SER} = -1677948.15 + 1312 * T - 192.46 * T * LN(T)$	
${}^0G_{Al^{3+}:O^{2-},VA}^L = +252595.12 - 41.74 * T$	
Al <sub>2</sub> O <sub>3</sub> : Model (Al <sup>3+</sup> ) <sub>2</sub> (O <sup>2-</sup> ) <sub>3</sub>	
${}^0G^{MgO} - H_{Mg}^{SER} - H_O^{SER} = -1723232.33 + 749 * T - 115.79 * T * LN(T)$	

solid MgO phase, as well as the stability diagram of the Mg-O system. In Fig. 1 (a), the calculated melting point of Mg was 923 K, which was the same as the result of Hallstedt [21]. “L1” corresponded to the Mg-rich liquid and “L2” corresponded to the MgO-rich liquid. The boiling point of Mg calculated in the present work was 1387 K which was higher than the calculated results by Hallstedt [21] (1373 K). This was the result of the update of the SGTE substance database [33]. The calculated melting point of the MgO was 3249 K, which was very close to the experimental data 3250±20 K. It can be concluded that the calculated phase diagram can reproduce the experiment data reasonably. As can be seen in Fig. 1 (b), the calculated enthalpy of formation of MgO was -300.62 kJ/mol-atoms which reproduced the experimental data well. Fig. 1 (c) shows the calculated heat capacity of MgO compared with the experimental data and the calculated result obtained from Hallstedt [21]. It was noted that the calculated heat capacity obtained from the present parameters agreed with the experimental data better.

Fig. 2 presents the calculated phase diagram of the Al-O system, enthalpy of formation and heat capacity of the solid Al<sub>2</sub>O<sub>3</sub> phase as well as the stability diagram of the Al-O system. The solubility of O in

liquid Al calculated by Otsuka and Kozuka [46] was considered in the present work. As seen in Fig. 2 (a), the calculated solubility of O in liquid Al reproduced the data from Otsuka and Kozuka [46] well. The calculated melting point of Al was 933 K which was the same as the result of Mao et al. [31]. “L1” corresponding to the Al-rich liquid and “L2” corresponding to the Al<sub>2</sub>O<sub>3</sub>-rich liquid. The boiling point of Al calculated in the present work was 2620 K which was consistent with the calculated result from Mao et al. [31]. Similarly, the reaction temperature of Gas=L1+Al<sub>2</sub>O<sub>3</sub>(s) was also lower based on the same reason. The calculated composition of the monotectic reaction near the melting of Al<sub>2</sub>O<sub>3</sub> was 59.1 at.% O, corresponding with the evaluated value 59.5±0.5 at.% O by Otsuka and Kozuka [46] well. The calculated temperature of the reaction was 2312 K, which was lower than the reported value by Schneider and McDaniel [69], but still within the error range. The melting point of Al<sub>2</sub>O<sub>3</sub> calculated in the present work was 2329 K. The calculated enthalpy of formation of Al<sub>2</sub>O<sub>3</sub> was -335.14 kJ/mol-atoms, which is consistent with the experimental data, as shown in Fig. 2(b). The calculated heat capacity of Al<sub>2</sub>O<sub>3</sub> shown in Fig. 2 (c) can reproduce the experimental data better than the calculated result from Mao et al. [31].

**Table 5.** Calculated thermodynamic properties of Mg-O and Al-O systems

	Enthalpy of formation (kJ/mol-atoms)	Standard entropy (J/mol•K)	Heat capacity at 298.15 K (kJ/mol- atoms)	Heat capacity of the liquid oxide (kJ/mol- atoms)	Enthalpy of melting (kJ/mol- atoms)
MgO	-300.62	28.1	18.65	33.47	53.41
Al <sub>2</sub> O <sub>3</sub>	-335.14	50.7	15.38	38.49	43.64



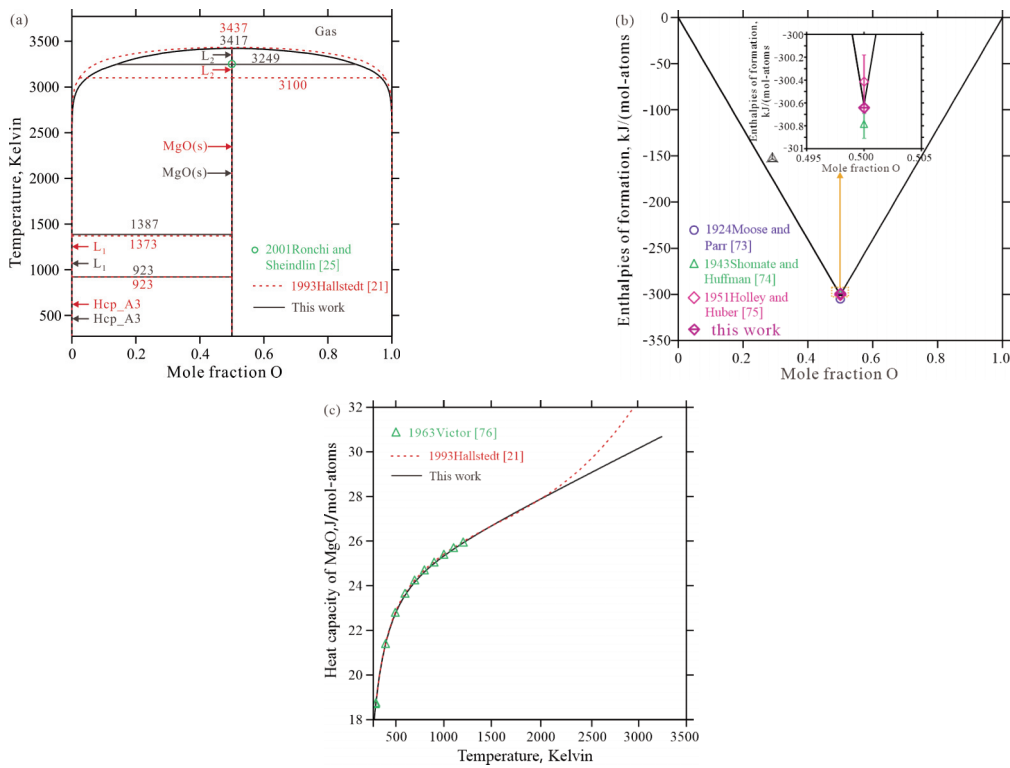


Figure 1. Calculated results of the Mg-O system compared with experimental data: (a) phase diagram; (b) enthalpy of formation of MgO; (c) heat capacity of MgO

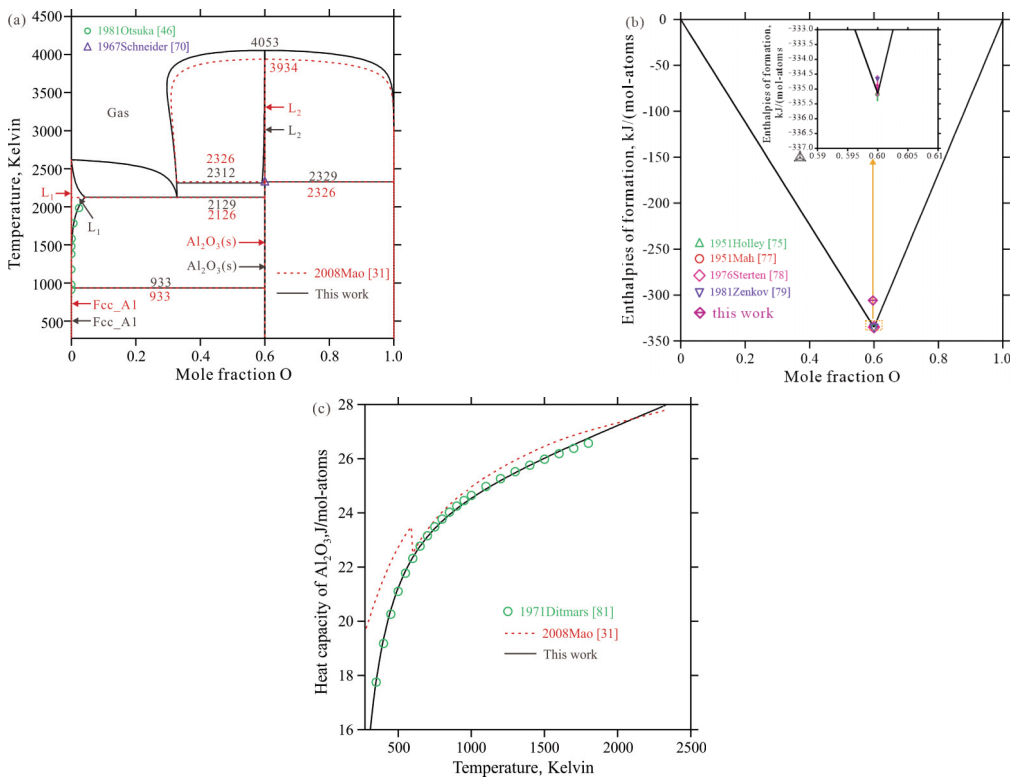


Figure 2. Calculated results of the Al-O system compared with experimental data: (a) phase diagram; (b) enthalpy of formation of Al<sub>2</sub>O<sub>3</sub>; (c) heat capacity of Al<sub>2</sub>O<sub>3</sub>



## 5. Conclusion

Phase diagram and thermodynamic properties of the Mg-O and Al-O systems were re-optimized by the CALPHAD method. The ionic liquid model was used to describe the liquid phase in the Mg-O and Al-O systems. For each system, a set of thermodynamic parameters was obtained. The calculated results using the presently obtained thermodynamic parameters can reproduce the experimental data well. Compared to the previous work in literature, the calculated thermodynamic parameters reproduce the phase diagram and thermodynamic properties more reasonably, especially for the heat capacity of MgO and Al<sub>2</sub>O<sub>3</sub>.

## Acknowledgement

*The financial support from the National Natural Science Foundation of China (Grant No. 51771235) is greatly acknowledged.*

## Author contributions

*Writing-original draft, Investigation, Data curation: Xiaojing Li. Funding acquisition, Writing-review & editing: Shuhong Liu.*

## Data availability

*The data used to support the findings of this study are available from the corresponding author upon request.*

## Conflict of interest

*The authors declare that they have no known competing financial interests or personal relationships that could have appeared to influence the work reported in this paper.*

## References

- [1] G.L. Song, A. Atrens, Corrosion mechanisms of magnesium alloys, *Advanced Engineering Materials*, 1 (1999) 11-33. [https://doi.org/10.1002/\(SICI\)1527-2648\(199909\)1:1<11::AID-ADEM11>3.0.CO;2-N](https://doi.org/10.1002/(SICI)1527-2648(199909)1:1<11::AID-ADEM11>3.0.CO;2-N).
- [2] A. Pardo, M.C. Merino, A.E. Coy, F. Viejo, R. Arrabal, S. Feliú, Influence of microstructure and composition on the corrosion behaviour of Mg/Al alloys in chloride media, *Electrochimica Acta*, 53 (2008) 7890-7902. <https://doi.org/10.1016/j.electacta.2008.06.001>.
- [3] J.R. Li, Q.T. Jiang, H.Y. Sun, Y.T. Li, Effect of heat treatment on corrosion behavior of AZ63 magnesium alloy in 3.5 wt.% sodium chloride solution, *Corrosion Science*, 111 (2016) 288-301. <https://doi.org/10.1016/j.corsci.2016.05.019>.
- [4] M. Esmaily, J.E. Svensson, S. Fajardo, N. Birbilis, G.S. Frankel, S. Virtanen, R. Arrabal, S. Thomas, L.G. Johansson, Fundamentals and advances in magnesium alloy corrosion, *Progress in Materials Science*, 89 (2017) 92-193. <https://doi.org/10.1016/j.pmatsci.2017.04.011>.
- [5] T.C. Xu, Y. Yang, X.D. Peng, J.F. Song, F.S. Pan, Overview of advancement and development trend on magnesium alloy, *Journal of Magnesium and Alloys*, 7 (2019) 536-544. <https://doi.org/10.1016/j.jma.2019.08.001>.
- [6] O. Lunder, T.K. Aune, K. Nisancioglu, Effect of Mn additions on the corrosion behavior of mould-cast magnesium ASTM AZ91, *Corrosion*, 43 (1987) 291-295. <https://doi.org/10.5006/1.3583151>.
- [7] G.L. Song, Recent progress in corrosion and protection of magnesium alloys, *Advanced Engineering Materials*, 7 (2005) 563-586. <https://doi.org/10.1002/adem.200500013>.
- [8] R.C. Zeng, J. Zhang, W.-J. Huang, W. Dietzel, K.U. Kainer, C. Blawert, W. Ke, Review of studies on corrosion of magnesium alloys, *Transactions of Nonferrous Metals Society of China*, 16 (2006) s763-s771. [https://doi.org/10.1016/S1003-6326\(06\)60297-5](https://doi.org/10.1016/S1003-6326(06)60297-5).
- [9] A. Atrens, G.L. Song, F.Y. Cao, Z.M. Shi, P.K. Bowen, Advances in Mg corrosion and research suggestions, *Journal of Magnesium and Alloys*, 1 (2013) 177-200. <https://doi.org/10.1016/j.jma.2013.09.003>.
- [10] M. Santamaria, F.D. Quarto, S. Zanna, P. Marcus, Initial surface film on magnesium metal: A characterization by X-ray photoelectron spectroscopy (XPS) and photocurrent spectroscopy (PCS), *Electrochimica Acta*, 53 (2007) 1314-1324. <https://doi.org/10.1016/j.electacta.2007.03.019>.
- [11] S. Feliu, C. Maffiotte, A. Samaniego, J.C. Galván, V. Barranco, Effect of naturally formed oxide films and other variables in the early stages of Mg-alloy corrosion in NaCl solution, *Electrochimica Acta*, 56 (2011) 4554-4565. <https://doi.org/10.1016/j.electacta.2011.02.077>.
- [12] S. Feliu, C. Maffiotte, A. Samaniego, J.C. Galván, V. Barranco, Effect of the chemistry and structure of the native oxide surface film on the corrosion properties of commercial AZ31 and AZ61 alloys, *Applied Surface Science*, 257 (2011) 8558-8568. <https://doi.org/10.1016/j.apsusc.2011.05.014>.
- [13] D. Wang, J.S. Zhang, J.D. Xu, Z.L. Zhao, W.L. Cheng, C.X. Xu, Microstructure and corrosion behavior of Mg-Zn-Y-Al alloys with long-period stacking ordered structures, *Journal of Magnesium and Alloys*, 2 (2014) 78-84. <https://doi.org/10.1016/j.jma.2014.01.008>.
- [14] L. Wang, T. Shinohara, B.-P. Zhang, XPS study of the surface chemistry on AZ31 and AZ91 magnesium alloys in dilute NaCl solution, *Applied Surface Science*, 256 (2010) 5807-5812. <https://doi.org/10.1016/j.apsusc.2010.02.058>.
- [15] M. Liu, S. Zanna, H. Ardelean, I. Frateur, P. Schmutz, G.L. Song, A. Atrens, P. Marcus, A first quantitative XPS study of the surface films formed, by exposure to water, on Mg and on the Mg-Al intermetallics: Al<sub>3</sub>Mg<sub>2</sub> and Mg<sub>17</sub>Al<sub>12</sub>, *Corrosion Science*, 51(5) (2009) 1115-1127. <https://doi.org/10.1016/j.corsci.2009.02.017>.
- [16] N. Saunders, A review and thermodynamic assessment of the Al-Mg and Mg-Li systems, *Calphad*, 14 (1990) 61-70. [https://doi.org/10.1016/0364-5916\(90\)90040-7](https://doi.org/10.1016/0364-5916(90)90040-7).
- [17] P. Liang, T. Tarfa, J.A. Robinson, S. Wagner, P. Ochin, M.G. Harmelin, H.J. Seifert, H.L. Lukas, F. Aldinger, Experimental investigation and thermodynamic



- calculation of the Al-Mg-Zn system, *Thermochimica Acta*, 314 (1998) 87-110.  
[https://doi.org/10.1016/S0040-6031\(97\)00458-9](https://doi.org/10.1016/S0040-6031(97)00458-9).
- [18] Y. Zhong, M. Yang, Z.-K. Liu, Contribution of first-principles energetics to Al-Mg thermodynamic modeling, *Calphad*, 29 (2005) 303-311.  
<https://doi.org/10.1016/j.calphad.2005.08.004>.
- [19] H.A. Wriedt, The Mg-O (magnesium-oxygen) system, *Bulletin of Alloy Phase Diagrams*, 8 (1987) 227-233.  
<https://doi.org/10.1007/BF02874914>.
- [20] H.A. Wriedt, The Al-O (aluminum-oxygen) system, *Bulletin of Alloy Phase Diagrams*, 6 (1985) 548-553.  
<https://doi.org/10.1007/BF02887157>.
- [21] B. Hallstedt, Thermodynamic calculation of some subsystems of the Al-Ca-Mg-Si-O system, *Journal of Phase Equilibria*, 14 (1993) 662-675.  
<https://doi.org/10.1007/BF02667878>.
- [22] S.-M. Liang, R. Schmid-Fetzer, Complete thermodynamic description of the Mg-Ca-O phase diagram including the Ca-O, Mg-O and CaO-MgO subsystems, *Journal of the European Ceramic Society*, 38 (2018) 4768-4785.  
<https://doi.org/10.1016/j.jeurceramsoc.2018.06.015>.
- [23] S. Ma, F.Z. Xing, N. Ta, L.J. Zhang, Kinetic modeling of high-temperature oxidation of pure Mg, *Journal of Magnesium and Alloys*, 8 (2020) 819-831.  
<https://doi.org/10.1016/j.jma.2019.12.005>.
- [24] A.P. Chernyshev, V.A. Petrov, V.E. Titov, A.Y. Vorobyev, Thermal radiative properties of magnesium oxide at high temperatures, *Thermochimica Acta*, 218 (1993) 195-209.  
[https://doi.org/10.1016/0040-6031\(93\)80422-7](https://doi.org/10.1016/0040-6031(93)80422-7).
- [25] C. Ronchi, M. Sheindlin, Melting point of MgO, *Journal of Applied Physics*, 90 (2001) 3325-3331.  
<https://doi.org/10.1063/1.1398069>.
- [26] I.I. Vol'nov, S.A. Tokareva, V.N. Belevskii, E.I. Latysheva, The formation of magnesium peroxide  $Mg(O_2)_2$  in the reaction of magnesium peroxide with ozone, *Izvestiia Akademiia Nauk SSSR Seriya Khimicheskaya*, 3 (1970) 513-516.
- [27] M. Blumenthal, Thermal dissociation of some peroxides and oxides. V. Thermal dissociation of magnesium, strontium and barium peroxides *roczniki*, *Zeitschrift für Anorganische Chemie*, 13 (1933) 5-15.
- [28] I.I. Vol'nov, Peroxides, superoxides, and ozonides of alkali and alkaline earth metals, *Nauka Moscow*, (1964).
- [29] O. Ruff, Arbeiten im Gebiet hoher Temperaturen I. Über das Schmelzen und Verdampfen unserer feuerbeständigsten Oxyde im elektrischen Vakuumofen, *Zeitschrift für Anorganische Chemie*, 82 (1913) 373-400.  
<https://doi.org/10.1002/zaac.19130820131>.
- [30] J.R. Taylor, A.T. Dinsdale, M. Hillert, M. Selleby, A critical assessment of thermodynamic and phase diagram data for the Al-O system, *Calphad*, 16 (1992) 173-179.  
[https://doi.org/10.1016/0364-5916\(92\)90005-I](https://doi.org/10.1016/0364-5916(92)90005-I).
- [31] H. Mao, M. Selleby, O. Fabrichnaya, Thermodynamic reassessment of the  $Y_2O_3$ - $Al_2O_3$ - $SiO_2$  system and its subsystems, *Calphad*, 32 (2008) 399-412.  
<https://doi.org/10.1016/j.calphad.2008.03.003>.
- [32] N. Ta, L. Zhang, Q. Li, Z. Lu, Y. Lin, High-temperature oxidation of pure Al: Kinetic modeling supported by experimental characterization, *Corrosion Science*, 139 (2018) 355-369.  
<https://doi.org/10.1016/j.corsci.2018.05.013>.
- [33] SGTE substances database, Scientific Group Thermodata Europe, Saint Martin d'Hères, France, 2013.
- [34] R. Minami, T. Nakajima, N. Watanabe, Emulsions in molten salts. Dispersion of magnesium metal in molten magnesium chloride-potassium chloride, *Nippon Kagaku Kaishi*, 11 (1975) 1892-1895.  
<https://doi.org/10.1246/bcsj.47.2071>.
- [35] K. Schwitzgebel, P.S. Lowell, Thermodynamic basis for existing experimental data in Mg- $SO_2$ - $O_2$  and Ca- $SO_2$ - $O_2$  systems, *Environmental Science & Technology*, 7 (1973) 1147-1151.  
<https://doi.org/10.1021/es60085a001>.
- [36] C.W. Kanolt, The melting points of some refractory oxides, *Journal of the Washington Academy of Sciences*, 3 (1913) 315-318.  
<https://doi.org/10.6028/bulletin.232>.
- [37] R.N. McNally, F.I. Peters, P.H. Ribbe, Laboratory furnace for studies in controlled atmospheres: Melting points of MgO in a  $N_2$  atmosphere and of  $Cr_2O_3$  in  $N_2$  and in air atmospheres, *Journal of the American Society*, 44 (1961) 491-493.  
<https://doi.org/10.1111/j.1151-2916.1961.tb13711.x>.
- [38] B. Riley, The determination of melting points at temperatures above 2000 Celsius, *Revue Internationale des Hautes Temperatures et des Refractaires*, 3 (1966) 327-336.  
<https://doi.org/10.1088/0950-7671/41/8/406/meta>.
- [39] J. Czochralski, The Solubility of Gases in Aluminum, *Zeitschrift für Metallkunde*, 14 (1922) 277-285.
- [40] G. Jander, W. BrSsse, Quantitative separations and determinations through volatilization with hydrogen chloride. 6th report: On the quantitative determination of the oxygen content of aluminum alloys, *Zeitschrift für Anorganische Chemie*, 41 (1928) 702-704.
- [41] H. Lowenstein, On the oxygen content of aluminum and methods for its determination, *Zeitschrift für Anorganische Chemie*, 199 (1931) 48-56.
- [42] R. Sterner-Rainer, On the occurrence of small amounts of gases and oxides in aluminum and Al-alloys, *Zeitschrift für Metallkunde*, 23 (1931) 274-282.
- [43] H.A. Sloman, The application of the vacuum fusion method to the determination of the oxygen, hydrogen and nitrogen contents of non-ferrous metals, alloys and powders, *Journal of the Institute of Metals*, 71 (1945) 391-414.
- [44] H. Schmitt, H. Wittner, Origin of the nonmetallic impurities in aluminum and their influence on its further working, *Zeitschrift Erzbergbau Metals*, 9 (1956) 417-421.
- [45] D. Gibbons, E.S. G. Olive, J.E. Deutschman, Determination of the oxygen content of aluminum by 14 MeV-Neutron radioactivation analysis, *Journal of the Institute of Metals*, 95 (1967) 280-283.
- [46] S. Otsuka, Z. Kozuka, Thermodynamic study of oxygen in liquid elements of group Ib to VIb, *Transactions of the Japan Institute of Metals*, 22 (1981) 558-566.  
<https://doi.org/10.2320/matertrans1960.22.558>.
- [47] O. Ruff, O. Goecke, Effect of environment upon the melting point of  $Al_2O_3$ , *Zeitschrift für Anorganische Chemie*, 24 (1911) 1459-1465.
- [48] C.W. Kanolt, Melting points of fire bricks, *Bulletin of*



- alloy phase diagrams, 10 (1914) 295-313.
- [49] E. Tiede, E. Birnbrauer, Spezielle arbeitsmethoden zur erzeugung hoher temperaturen im vakuum und das verhalten einiger metalle, oxyde und carbide bei denselben, Zeitschrift für Anorganische Chemie, 87 (1914) 129-168.
- [50] O. Ruff, G. Lauschke, Zeitschrift für Anorganische Chemie, 97 (1916) 73-113.
- [51] H.V. Wartenberg, H. Linde, R. Jung, Melting-point curve of refractory oxides, Zeitschrift für Anorganische Chemie, 176 (1928) 349-362. [https://doi.org/10.1016/s0016-0032\(13\)90732-8](https://doi.org/10.1016/s0016-0032(13)90732-8).
- [52] E.N. Bunting, Journal of Research of the National Bureau of Standards 6 (1931).
- [53] O. Weigel, F. Kaysser, Neues Jahrbuch für Mineralogie, 64 (1931) 321-396.
- [54] R.F. Geller, E.N. Bunting, Report on the systems lead oxide-alumina and lead oxide-alumina-silica, Journal of Research of the National Bureau of Standards, 31 (1943) 255-270. <https://doi.org/10.6028/jres.031.015>.
- [55] R.F. Geller, P.J. Yavorsky, Melting point of alpha-alumina, Journal of Research of the National Bureau of Standards, 34 (1945) 395-401. <https://doi.org/10.6028/jres.034.021>
- [56] W.A. Lambertson, F.H. Gunzel, Compilation of melting points of the metal oxides, U.S. AEC Public AEC-D, 3465 (1952) 1-4. <https://doi.org/10.6028/nbs.mono.68>.
- [57] S.M. Lang., F.P. Knudsen, C.L. Filmore, R.S. Roth, National Bureau of Standards of Circulation, 568 (1956) 1-32.
- [58] F.H. Aldred, H.E.S. White, Some equipment for ceramic research, Transactions and Journal of the British Ceramic Society, 58 (1959) 199-223.
- [59] S.D. Mark, Note on the system magnesia-thoria-hafnia, Journal of the American Ceramic Society, 42 (1959) 208. <https://doi.org/10.1111/j.1151-2916.1959.tb12949.x>.
- [60] J.J. Diamond, S.J. Schneider, Apparent temperatures measured at melting points of some metal oxides in a solar furnace, Journal of the American Ceramic Society, 43 (1960) 1-3. <https://doi.org/10.1111/j.1151-2916.1960.tb09143.x>.
- [61] V.Y. Chekhovskoi, V.A. Petrov, Melting point of corundum, Thermotechnical Measurements, 9 (1963) 26-28. <https://doi.org/10.1007/BF01419351>.
- [62] W. Gutt., A microfurnace for high temperature microscopy and X-ray analysis up to 2150 °C, Journal of Scientific Instruments, 41 (1964) 393-394. <https://doi.org/10.1088/0950-7671/41/6/415/meta>.
- [63] B. Riley, A method for accurate melting point determination at high temperatures, Journal of Scientific Instruments, 41 (1964) 504-505. <https://doi.org/10.1088/0950-7671/41/8/406/meta>.
- [64] M. Foex, Measurement of the solidification points of several refractory oxides by means of a solar furnace, Solar Energy, 9 (1965) 61-67. [https://doi.org/10.1016/0038-092x\(65\)90162-3](https://doi.org/10.1016/0038-092x(65)90162-3).
- [65] G. Gitlesen, K. Motzfeldt, The melting point of alumina and some related observations, Acta Chemica Scandinavica, 19 (1965) 661-669.
- [66] P.B. Kantor, E.N. Fomichev, V.V. Kandyba, Melting point of corundum as a secondary reference point of the temperature scale, Izmerit Technology, 5 (1966) 27-29.
- [67] T. Sata, Measurement of the melting point of pure oxides utilizing small samples, revue, Internationale des Hautes Temperatures et des Refractaires, 3 (1966) 337-341.
- [68] G. Urbain, M. Rouannet, Secondary points of reference in the practical scale of temperatures, experimental determination of the temperature of fusion of alumina, Revue International des Hautes Temperatures et des Refractaires, 3 (1966) 363-369. <https://doi.org/10.6028/jres.065a.017>.
- [69] S.J. Schneider, C.L. McDaniel, Effect of environment upon the melting point of Al<sub>2</sub>O<sub>3</sub>, Journal of Research of the National Bureau of Standards-A. Physics and Chemistry, 71A (1967) 317-333. <https://doi.org/10.6028/jres.071a.038>.
- [70] M.W. Chase, J.L. Curnutt, R.A. McDonald, A.N. Syverud, JANAF thermochemical tables, 1978 supplement, Journal of Physical and Chemical Reference Data, 7 (1978) 793-940. <https://doi.org/10.1063/1.3253143>.
- [71] L.B. Pankratz, Thermodynamic properties of elements and oxides, U.S. Department of the Interior, Bureau of Mines, (1982).
- [72] J.E. Moose, S.W. Parr, A re-determination of the heats of oxidation of certain metals, Heats of Oxidation of Metals, 46 (1924) 2656-2661. <https://doi.org/10.1021/ja01677a007>.
- [73] C.H. Shomate, E.H. Huffman, Heat of formation of MgO, MgCl<sub>2</sub>, MgCl<sub>2</sub>·H<sub>2</sub>O, MgCl<sub>2</sub>·2H<sub>2</sub>O, MgCl<sub>2</sub>·4H<sub>2</sub>O, and MgCl<sub>2</sub>·6H<sub>2</sub>O, Trimethylamine Compounds with Sulfur Dioxide, 65 (1943) 1625-1629. <https://doi.org/10.1021/ja01248a048>.
- [74] C.E. Holley, E.J. Huber, The heats of combustion of magnesium and aluminum, Journal of the American Chemical Society, 73 (1951) 5577-5579. <https://doi.org/10.1021/ja01156a020>.
- [75] A.C. Victor, T.B. Douglas, Thermodynamic properties of magnesium oxide and beryllium oxide from 298 to 1200 K, Journal of Research of the National Bureau of Standards, 67A (1963) 325-329. <https://doi.org/10.6028/jres.067a.034>.
- [76] A.D. Mah, Heats of formation of alumina, molybdenum trioxide and molybdenum dioxide, Journal of Physical Chemistry, 61 (1957) 1572-1573. <https://doi.org/10.1021/j150557a028>.
- [77] A. Sterten, S. Haugen, K. Hamberg, The NaF-AlF<sub>3</sub>-Al<sub>2</sub>O<sub>3</sub>-Na<sub>2</sub>O system—I standard free energy of formation of α-aluminium oxide from emf measurements, Electrochimica Acta, 21 (1976) 589-592. [https://doi.org/10.1016/0013-4686\(76\)85154-7](https://doi.org/10.1016/0013-4686(76)85154-7).
- [78] I.D. Zenkov, Calorimetric method of determining degree of crystallinity of cellulosic materials Journal of Physical Chemistry, 55 (1981) 1698-1702. <https://doi.org/10.1007/bf00545388>.
- [79] D.A. Ditmars, T.B. Douglas, Measurement of the relative enthalpy of pure α-Al<sub>2</sub>O<sub>3</sub> (NBS heat capacity and enthalpy standard reference material No. 720) from 273 to 1173 K, Journal of Research of the National Institute of Standards and Technology, 75A (1971) 401-420. <https://doi.org/10.6028/jres.075A.031>
- [80] D.A. Ditmars, S. Ishihara, S.S. Chang, G. Bernstein, Enthalpy and heat-capacity standard reference material: synthetic sapphire (α-Al<sub>2</sub>O<sub>3</sub>) from 10 to 2250 K, Journal of Research of the National Bureau of Standards, 87 (1982) 159-163. <https://doi.org/10.6028/jres.087.012>.



- [81] A.T. Dinsdale, SGTE data for pure elements, Calphad, 15 (1991) 317-425.  
[https://doi.org/10.1016/0364-5916\(91\)90030-N](https://doi.org/10.1016/0364-5916(91)90030-N).
- [82] M. Hillert, B. Jansson, B. Sundman, J. Ågren, A two-sublattice model for molten solutions with different tendency for ionization, Metallurgical Transactions A, 16A (1985) 261-266.  
<https://doi.org/10.1007/BF02815307>.
- [83] B. Sundman, Modification of the two-sublattice model for liquids, Calphad, 15 (1991) 109-119.  
[https://doi.org/10.1016/0364-5916\(91\)90010-H](https://doi.org/10.1016/0364-5916(91)90010-H).
- [84] <http://www.crystallography.net/cod/>.
- [85] P. Hohenberg, W. Kohn, Inhomogeneous electron gas, Physical Review 136 (1964) 864-871.  
<https://doi.org/10.1103/physrev.136.b864>.
- [86] W. Kohn, L.J. Sham, Self-consistent equations including exchange and correlation effects, Physical Review 140 (1965) A1133-A1138.  
<https://doi.org/10.1103/physrev.140.a1133>.
- [87] G. Kresse, J. Furthmüller, Efficiency of ab-initio total energy calculations for metals and semiconductors using a plane-wave basis set, Computational Materials Science 6 (1996) 15-50.  
[https://doi.org/10.1016/0927-0256\(96\)00008-0](https://doi.org/10.1016/0927-0256(96)00008-0).
- [88] G. Kresse, J. Furthmüller, Efficient iterative schemes for ab initio total-energy calculations using a plane-wave basis set, Physical Review B, 54 (1996) 11169-11186.  
<https://doi.org/10.1103/PhysRevB.54.11169>.
- [89] G. Kresse, D. Joubert, From ultrasoft pseudopotentials to the projector augmented-wave method, Physical Review B, 59 (1996) 1758-1775.  
<https://doi.org/10.1103/physrevb.59.1758>.
- [90] J.P. Perdew, K. Burke, M. Ernzerhof, Generalized gradient approximation made simple, Physical Review Letter, 77 (1996) 3865-3868.  
[https://doi.org/S0031-9007\(96\)01479-2](https://doi.org/S0031-9007(96)01479-2).
- [91] B. Sundman, B. Jansson, J.O. Andersson, The ThermoCalc databank system, Calphad, 9 (1985) 153-190.  
[https://doi.org/10.1016/0364-5916\(85\)90021-5](https://doi.org/10.1016/0364-5916(85)90021-5).
- [92] Y. Du, R. Schmid-Fetzer, H. Ohtani, Thermodynamic assessment of the V-N system, Zeitschrift für Metallkunde, 88 (1997) 545-556.  
<https://doi.org/10.3139/ijmr-1997-0101>.
- [93] Y. Du, S.H. Liu, L.J. Zhang, H.H. Xu, D.D. Zhao, A.J. Wang, L.C. Zhou, An overview on phase equilibria and thermodynamic modeling in multicomponent Al alloys: Focusing on the Al-Cu-Fe-Mg-Mn-Ni-Si-Zn system, Calphad, 35 (2011) 427-445.  
<https://doi.org/10.1016/j.calphad.2011.06.007>.

## TERMODINAMIČKI OPIS Mg-O I Al-O SISTEMA

X.-J. Li, S.-H. Liu\*

Centralni južni univzitet, Glavna državna laboratorija za nauku i tehnologiju visoko-čvrstih strukturnih materijala, Čangša, Hunan, Kina

### Apstrakt

Termodinamička svojstva oksida značajno utiču na koroziono ponašanje legura. MgO i Al<sub>2</sub>O<sub>3</sub> su važni proizvodi u procesu korozije Mg-Al legura, stoga je neophodno istražiti njihova termodinamička svojstva. Mg-O i Al-O sistemi su kritički procenjeni i reevaluirani primenom CALPHAD (CALculation of PHase Diagram) pristupa. Tečne faze ovih sistema su opisane korišćenjem modela jonske težnosti. Prema podacima iz literature, oksidne faze, MgO i Al<sub>2</sub>O<sub>3</sub>, tretirani su kao stehiometrijska jedinjenja. Termodinamički parametri ova dva stehiometrijska jedinjenja su optimizovani uzimajući u obzir i fazni dijagram i termodinamičke podatke, i na kraju je određen skup samokonzistentnih termodinamičkih parametara za svaki sistem. Izračunati rezultati korišćenjem trenutno dobijenih termodinamičkih parametara mogu razumno reprodukovati pouzdane eksperimentalne podatke iz literature.

**Ključne reči:** Mg-O; Al-O; Termodinamička evaluacija; Fazni dijagram; CALPHAD metoda

